ACS Medicinal Chemistry Letters

Letter

pubs.acs.org/acsmedchemlett

Discovery of Pyrazolopyridones as a Novel Class of Gyrase B Inhibitors Using Structure Guided Design

Jason B. Cross,*[,†] Jing Zhang,[†] Qingyi Yang,[†] Michael F. Mesleh,[†] Jan Antoinette C. Romero,[†] Bin Wang,[†] Doug Bevan,[†] Katherine M. Poutsiaka,[†] Felix Epie,[†] Terence Moy,[†] Anu Daniel,[†] Joseph Shotwell,[†] Brian Chamberlain,[†] Nicole Carter,[†] Ole Andersen,[‡] John Barker,[‡] M. Dominic Ryan,[†] Chester A. Metcalf, III,[†] Jared Silverman,[†] Kien Nguyen,[†] Blaise Lippa,[†] and Roland E. Dolle[†]

[†]Cubist Pharmaceuticals, Inc., 65 Hayden Avenue, Lexington, Massachusetts 02421, United States

[‡]Evotec U.K., Ltd., 114 Innovation Drive, Milton Park, Abingdon, Oxfordshire OX14 4RZ, United Kingdom

Supporting Information

ABSTRACT: The ATPase subunit of DNA gyrase B is an attractive antibacterial target due to high conservation across bacteria and the essential role it plays in DNA replication. A novel class of pyrazolopyridone inhibitors was discovered by optimizing a fragment screening hit scaffold using structure guided design. These inhibitors show potent Gram-positive antibacterial activity and low resistance incidence against clinically important pathogens.

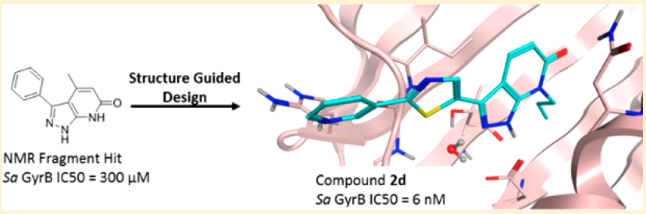

KEYWORDS: *Antibacterials, DNA gyrase B, fragment-based drug design, structure-based drug design*

Bacterial DNA gyrase is the molecular target for the clinically important fluoroquinolone drug class, making it a highly valuable target for antibacterial research.[1] Functionally, DNA gyrase exists as an A_2B_2 tetramer that binds dsDNA and catalyzes strand breakage/reformation that leads to the introduction of negative supercoils.[2,3] Novel chemotypes that bind to other regions of the protein complex would have the advantage of avoiding on-target fluoroquinolone resistance mechanisms. Inhibition of the ATPase activity of the GyrB subunit is known to block bacterial DNA replication, resulting in potent antibacterial activity.[4−9] There is high sequence and structural homology between GyrB and the ParE subunit of topoisomerase IV, which presents the possibility of dual-targeting that is expected to lead to improved bacterial resistance. As a result, there has been considerable interest in targeting both GyrB and ParE simultaneously.[5,6,8,9]

Identification of novel scaffolds with antibacterial activity using synthetic library screening approaches, i.e., high-throughput screening, has yielded few tractable lead compounds, despite large-scale screening campaigns conducted by pharmaceutical companies.[10] An alternate strategy for hit identification is fragment-based drug design (FBDD). This technique has been used successfully to find novel hits in several therapeutic areas, including antibacterials.[9,11]

A fragment-based screen using NMR as the detection method was conducted to identify novel scaffolds that bind to the GyrB ATPase site. One of the most promising hits was a pyrazolopyridone, compound **1** (Figure 1a), chemically similar to a primary hit from the screen. Structure guided design techniques were used to improve the potency of the fragment hit, leading to a novel compound **2a**.[12]

An X-ray crystallographic structure of **2a** bound to a 24 kDa construct of *S. aureus* GyrB containing the ATPase domain (PDB ID 5CTY)[13] provided a reference for structure-based optimization of this scaffold. Several key binding interactions are highlighted in Figure 1b, with amino acid numbering based on the *Sa* sequence. A hydrogen bond donor−acceptor motif was clearly seen between the pyrazole of **2a**, the carboxylate side chain of Asp81 (Asp73 *Ec* numbering), and a conserved water molecule stabilized by hydrogen bonds to Asp81, Gly85, and Thr173 (*Ec* Asp73, Gly77, and Thr165, respectively). Lipophilic contacts were evident between the central thiazole and Ile86 (*Ec* Ile78). The pyridine ring stacked with Arg84 (*Ec* Arg76), forming a π−cation interaction, and also participated in a hydrogen bond with the cationic side chain of Arg144 (*Ec* Arg136). There was also a hydrogen bond formed between the pyridone carbonyl oxygen and the side chain of Asn54 (*Ec* Asn46). Trius reported that interaction with Asn54 was a critical feature of their tricyclic GyrB inhibitors, which greatly improved enzymatic and antibacterial activities.[14]

In addition to the protein−ligand interactions observed in the X-ray costructure with **2a**, there was also clear electron density for two water molecules deeply trapped in a small hydrophobic pocket between Ile51 and Ile175 (*Ec* Val43 and Val167). Water analysis using 3D-RISM (as implemented in MOE[15]) was performed on this X-ray structure with compound **2a** present and with compound **2a** removed (mimicking the apo protein). Analysis of the pseudoapo binding site (Figure

Received: September 20, 2015
Accepted: February 6, 2016

DOI: 10.1021/acsmedchemlett.5b00368
ACS Med. Chem. Lett. XXXX, XXX, XXX−XXX

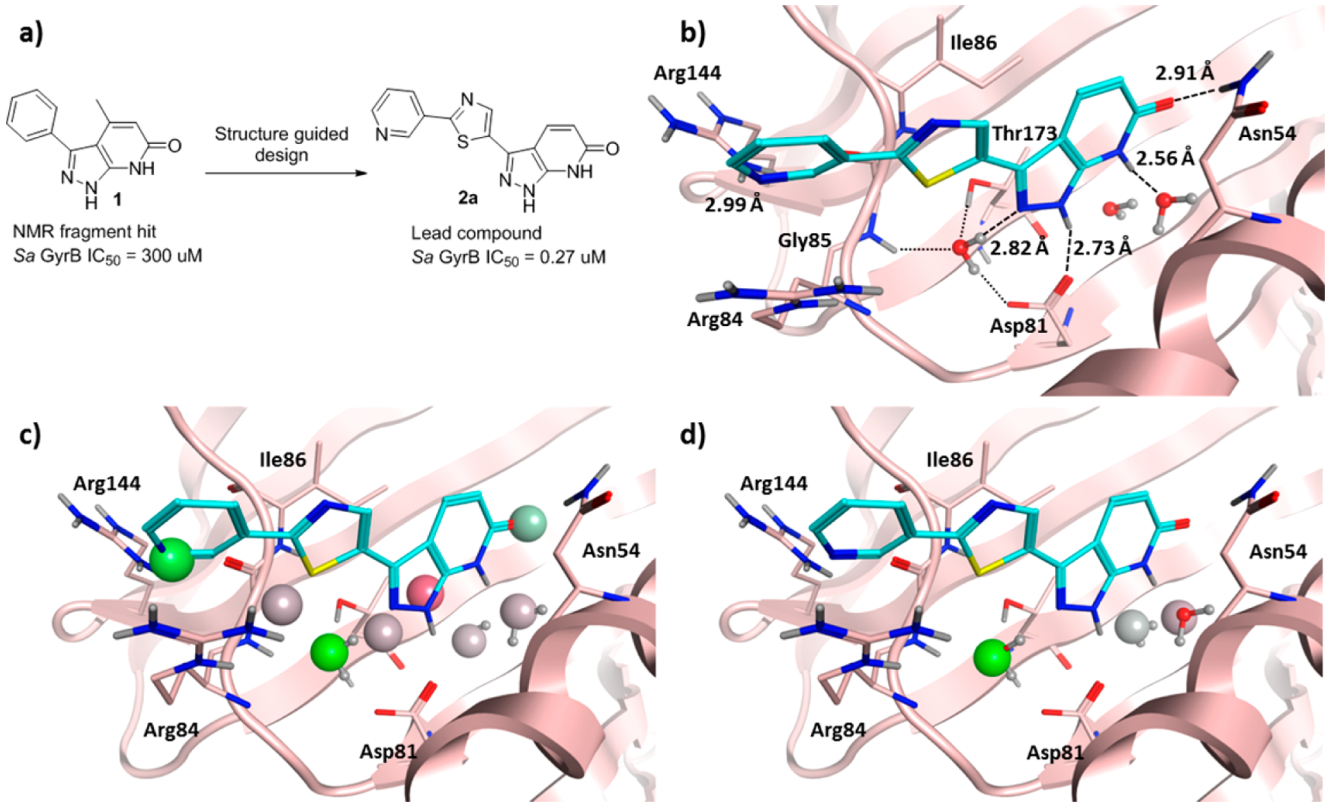

Figure 1. (a) Pyrazolopyridone fragment hit was transformed into a lead using structure guided design. (b) Key interactions between GyrB and the pyrazolopyridone scaffold (compound **2a**, cyan), including hydrogen bonds to Asp81, Asn54, Arg144, and water molecules, as well as a π−cation stacking interaction with Arg84 (*Sa* numbering). (c) 3D-RISM analysis of the GyrB ATPase site. Calculations were performed without a ligand occupying the active site; compound **2a** (cyan) was overlaid on the 3D-RISM results for clarity. Energetically favorable water molecules predicted using 3D-RISM are green, and energetically disfavored water molecules are red. (d) 3D-RISM analysis of the GyrB ATPase site with compound **2a** (cyan) present. An energetically favored water site (green sphere) overlays a tightly bound water molecule bound to Asp81, Gly85, and Thr173, while two poorly bound water sites (red/gray spheres) overlay water molecules in the hydrophobic binding site adjacent to Asn54. Graphics generated using MOE.[15]

1c) suggested that highly bound water molecules (green) should exist at the sites of the crystallographically conserved water molecule and at the nitrogen of the pyridine ring (calculated free energies of −19.8 and −6.1 kcal/mol, respectively). These results indicate that displacement of water from these positions is unlikely without very favorable compensatory protein−ligand interactions.

In addition, there were several water sites in the pseudoapo binding site that were predicted to have poorly bound water molecules (Figure 1c, red, pink, and gray). These included sites that overlapped the pyrazolopyridone (4.2 and 0.7 kcal/mol) and were within the van der Waals radius of the thiazole sulfur atom (1.0 kcal/mol), as well as the hydrophobic pocket (0.8 and 0.6 kcal/mol). Coverage of these regions of the active site, as in compound **2a**, resulted in nanomolar inhibition and a promising starting point for optimization.

Solvent analysis of the bound structure of compound **2a** showed that the water molecules in the hydrophobic pocket were still moderately or poorly bound in the presence of an inhibitor (1.0 and −0.2 kcal/mol), as seen in Figure 1d. This suggested an opportunity for improvement of binding affinity by displacing these water molecules.

Based on these analyses, structure-based optimization was undertaken to explore the SAR of the pyridone ring (Table 1). Scheme 1 outlines the synthesis of analogues with various substituents on the pyrazolopyridone ring. At the R^1 position, improvements in IC_{50} and whole cell activity (as measured by MICs against Sa42, a methicillin-susceptible *S. aureus* strain) correlated with *n*-alkyl extension into the hydrophobic pocket, consistent with the results of the 3D-RISM calculations.

Table 1. Enzymatic and in Vitro Antibacterial Activities of Pyrazolopyridone Analogues Containing Pyridone Substitutions

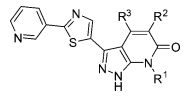

Cpd	R^1	R^2	R^3	*Sa* GyrB ATPase IC_{50} (μM)	*Sa*42 MSSA MIC (μg/mL)
Moxifloxacin					0.06
2a	H	H	H	0.270	>32
2b	Me	H	H	0.051	>32
2c	Et	H	H	0.020	2
2d	n-Pr	H	H	0.006	0.06
2e	Allyl	H	H	0.004	0.25
2f	CH_2CH_2OH	H	H	0.564	>32
2g	Et	Me	H	0.035	2
2h	Et	CH_2OH	H	0.202	>32
2i	Et	CONHMe	H	3.349	>32
2j	H	H	Me	3.248	ND
2k	H	H	Ph	1.315	ND

DOI: 10.1021/acsmedchemlett.5b00368
ACS Med. Chem. Lett. XXXX, XXX, XXX−XXX

Scheme 1. Synthetic Route for Varying Substituents on the Pyrazolopyridone Ring[a]

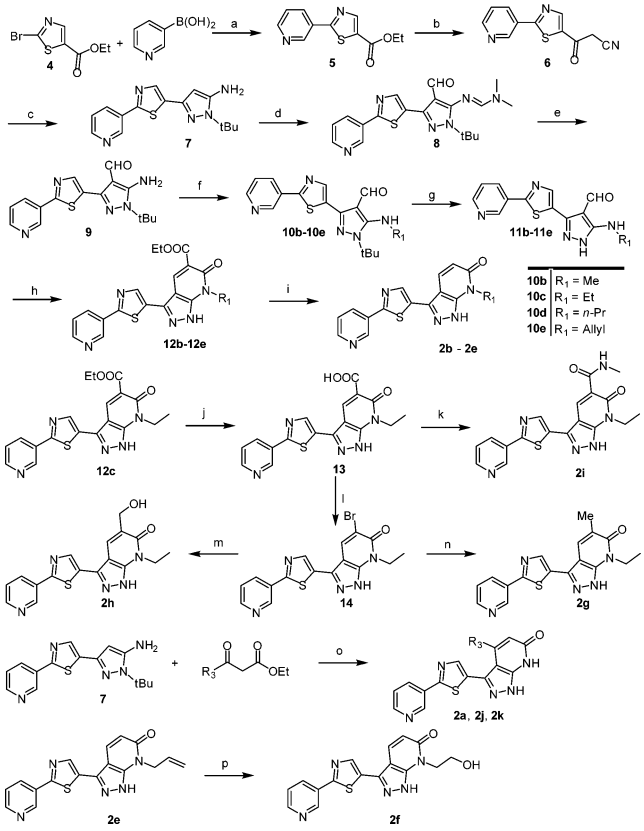

[a]Reagents and conditions: (a) $Pd(dppf)Cl_2$, dioxane, Na_2CO_3, 100 °C, 55%; (b) *n*-BuLi, CH_3CN, −78 °C, THF, 35%; (c) *t*-$BuNHNH_2$, NEt_3, *i*PrOH, 80 °C, 50%; (d) $POCl_3$, DMF, 70 °C, 100%; (e) 40% aq. NaOH, EtOH, 80 °C, 52%; (f) R_1X, Cs_2CO_3, DMF, RT; (g) TFA, 70 °C; (h) diethylmalonate, piperidine, EtOH, 80 °C; (i) 40% HBr, 140 °C, *mv*; (j) LiOH, THF/MeOH; (k) CH_3NH_2, HATU, DMF, 20%; (l) NBS, 25 °C, 87%; (m) $HOCH_2Sn(Bu)_3$, $Pd(PPh_3)_2Cl_2$, dioxane, *mv*, 120 °C, 10%; (n) $(MeBO)_3$, $Pd(dppf)Cl_2$, dioxane, Na_2CO_3, 110 °C, 12%; (o) 1. AcOH, 110 °C; 2. TFA, 70 °C; (p) 1. OsO_4, NMO, 53%; 2. $NaIO_4$, MeOH, 66%; 3. $NaBH_4$, MeOH, 33%.

Optimal enzymatic and whole cell potency for R^1 substitutions was achieved through incorporation of an *n*-propyl group (compound **2d**), resulting in complete displacement of water, as seen in a high resolution X-ray structure (Figure 2, PDB ID 5D7D). Introduction of an allyl group (compound **2e**) maintained activity in the enzymatic assay relative to compound **2d**, but resulted in poorer whole cell activity, while hydrophilic groups, such as hydroxyethyl (compound **2f**), were not tolerated.

The R^2 position only tolerated substitution of small groups, such as methyl (compound **2g**), which was consistent with the constricted binding pocket features observed in the *S. aureus* GyrB X-ray structures. Larger substitutions, including those with hydrophilic groups, had poor enzyme and whole cell activity.

Hydrogen at the R^3 position resulted in the best potency of the substitutions explored, due to the need for a small dihedral angle between the pyrazolopyridone and thiazole rings. Larger dihedral angles, caused by larger substituents at the R^3 position (compounds **2j** and **2k**), resulted in unfavorable interactions between the thiazole and lipophilic wall of the protein.[12]

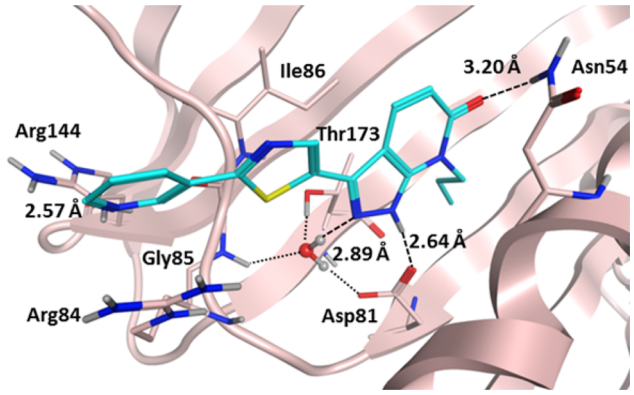

Figure 2. X-ray structure of compound **2d** bound to *S. aureus* GyrB (1.70 Å resolution; PDB ID 5D7D). The lipophilic pocket is filled by the *n*-propyl group attached to the pyridone. Graphics generated using MOE.[15]

Table 2 outlines a series of substitutions that were made at the 2-position of the pyridine group of compound **2d**, in order to modulate the physicochemical properties of the series, while Scheme 2 illustrates the route used for synthesis.

Table 2. Enzymatic and in Vitro Antibacterial Activities of Pyrazolopyridone Analogues Containing Pyridine Substitutions

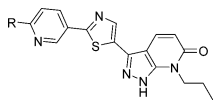

Cpd	R	*Sa* GyrB ATPase IC_{50} (uM)	*Sa*42 MSSA MIC (μg/mL)
3a	NMe_2	0.015	0.5
3b	4-methylpiperazine	0.008	2
3c	Me	<0.008	0.25
3d	CH_2OH	<0.008	0.25
3e	i-Pr	0.023	1
3f	CH_2-morpholine	<0.008	0.5
3g	CH_2-4-methylpiperazine	0.010	4
3h	CH_2NEt_2	0.009	4
3i	COOMe	0.015	0.5
3j	$CONMe_2$	0.008	2
3k	$CONHCH_2CH_2NEt_2$	<0.008	1
3l	$CONHCH_2CH_2$-morpholine	0.013	2

Consistent with the solvent exposed nature of pocket beyond the arginine interaction region, along with the 3D-RISM water analysis, the pyridine 2-position tolerated a variety of different chemical substitutions while maintaining enzymatic potency. However, whole cell activities were impacted by differences in the composition of the substituent. Small substituents, such as those of compounds **3a**, **3c**, and **3d**, generally had the best whole cell activity, but some larger substituents (compounds **3f** and **3i**) did result in reasonable MICs, albeit inconsistently. While substitutions in this region allowed exploration of physicochemical properties, including features such as charge state, hydrophobicity, and polar surface area, cheminformatics analyses showed little correlation between these properties and whole cell activity. This resulted in a design strategy that favored physicochemical property diversity and the use of

DOI: 10.1021/acsmedchemlett.5b00368
ACS Med. Chem. Lett. XXXX, XXX, XXX−XXX

Scheme 2. Synthetic Route for Pyridine Analogues[a]

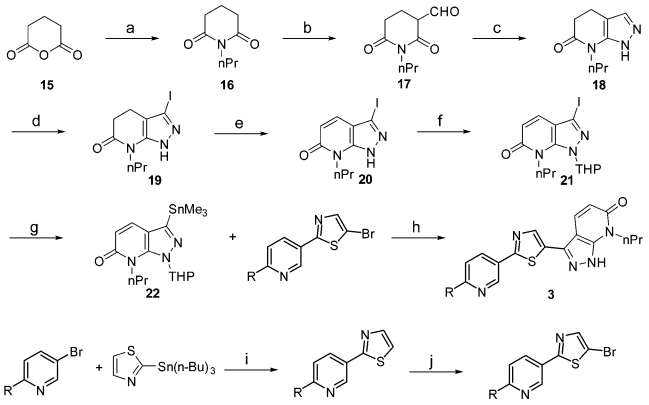

[a]Reagents and conditions: (a) *n*-PrNH$_2$, 130 °C, 50%; (b) *n*-BuLi, HCOOEt, THF, −78 °C; (c) NH$_2$NH$_2$, P$_2$O$_5$, EtOH, 80 °C, 25% over 2 steps; (d) NIS, DCE, 85 °C, 68%; (e) DDQ, dioxane, 110 °C, 99%; (f) Dihydropyran, TFA, 95 °C, 80%; (g) Pd(PPh$_3$)$_2$Cl$_2$, Me$_6$Sn$_2$, dioxane, 110 °C, 37%; (h) 1. Pd(PPh$_3$)$_2$Cl$_2$, P(furyl)$_3$, 100 °C; 2. TFA; (i) Pd(PPh$_3$)$_2$Cl$_2$, P(furyl)$_3$, 100 °C; (j) NBS, DMF.

structure-based design to drive improvements in ATPase inhibition.

The thiazolyl and pyridyl rings of compound **2d** were also varied to explore the SAR of this part of the scaffold (Table 3). Removal of the pyridyl ring (compound **4a**) resulted in a ∼50-fold loss in IC$_{50}$, underscoring the importance of the Arg84 and Arg144 interactions in enzymatic potency.

A regioisomer of the thiazolyl moiety was used to explore substitutions from this ring without significantly altering the electronic structure of this linker. Generally, moderately sized polar groups were tolerated in this position (e.g., compounds **4c** and **4d**), but this did not translate into robust whole cell activity.

Alternate linkers that replace the central thiazolyl ring were also explored using *in silico* scaffold replacement techniques.[15,16] Although linear and saturated ring linkers were somewhat tolerated, all compounds of this type suffered from decreased enzymatic activity and MICs. Care also had to be taken in the design of these compounds to ensure interactions in the arginine region of the pocket were maintained as the linker was varied. This often required simultaneous modification of the linker and tail group, as evidenced by compound **4e**.

Further characterization of compounds **2c** and **2d** was carried out against *Sa* ParE ATPase (Table 4). These compounds were chosen because they were available early in the program and, at the time, had the best MICs. Both compounds showed activity against *Sa* ParE, though they were 30- to 40-fold weaker against these enzyme subunits than *Sa* GyrB. Interaction with Ile86 (Ile78 in *Ec* GyrB), which is Met79 in *Sa* ParE, has been suggested by Charifson et al.[6] to contribute to dual activity. Since our compounds did not extend as far along this hydrophobic wall, ParE activity may have suffered. The weak ParE activity could be a contributing factor to the lower than expected RI observed for these compounds (∼10^{-9}), if they are considered single-target antibacterials; however, activity on another, unknown target cannot be ruled out as a cause.

The MICs for compounds **2c** and **2d** remained unchanged against a ciprofloxacin resistant MRSA strain (*Sa*1721 MRSA Cipro^R, Table 4). In comparison, moxifloxacin has a sizable MIC shift when tested against ciprofloxacin resistant MRSA (*Sa*1118 MRSA MIC = 0.06 μg/mL vs *Sa*1721 MRSA MIC > 2 μg/mL). This strongly suggests the site of action of the pyrazolopyridone compounds is not in the fluoroquinolone binding site and that target-based fluoroquinolone resistance mechanisms are not likely an issue for this class of inhibitor. Both compounds also displayed potent whole cell activity against other Gram-positive organisms, including *E. faecium* and *S. pneumoniae*, suggesting broad coverage of Gram-positives.

In conclusion, NMR-based fragment screening and hit follow-up identified pyrazolopyridone as a novel, active chemical scaffold against Sa GyrB. Medicinal chemistry efforts, guided by structure-based drug design, resulted in the discovery of pyrazolopyridone analogues with potent dual GyrB/ParE enzymatic activity, excellent resistance profiles, and broad spectrum Gram-positive antibacterial activity. The most potent analogue described herein, compound **2d**, showed whole cell activity against MRSA equivalent to that of moxifloxacin, while retaining activity against a ciprofloxacin resistant *S. aureus*

Table 3. Enzymatic and in Vitro Antibacterial Activities of Pyrazolopyridone Analogs with Linker (L) and Tail (R) Region Modifications

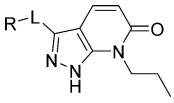

Cpd	R	L	*Sa* GyrB ATPase IC$_{50}$ (uM)	*Sa*42 MSSA MIC (μg/mL)
2d	3-Pyridyl	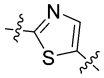	0.006	0.06
4a	H	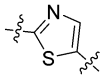	0.279	>32
4b	3-Pyridyl	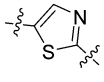	0.009	4
4c	3-Pyridyl		0.006	0.25
4d	3-Pyridyl		0.013	4
4e	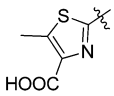	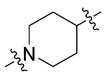	0.192	>32

Table 4. GyrB/ParE Activity and Resistance Profiles of Compound 2c and 2d

Cpd	2c	2d
Sa GyrB ATPase IC$_{50}$ (nM)	20	6
Sa ParE ATPase IC$_{50}$ (nM)	746	183
RI @ 4× MIC vs *Sa*	<10^{-9}	3 × 10^{-9}
MIC (μg/mL)		
*Sa*1118 MRSA	2	0.06
*Sa*1721 MRSA Cipro^R	4	0.06
E. faecium (ATCC 6569)	4	0.125
S. pneumonia (ATCC 6303)	4	0.25

DOI: 10.1021/acsmedchemlett.5b00368
ACS Med. Chem. Lett. XXXX, XXX, XXX−XXX

strain. Overall, the in vitro profile of the pyrazolopyridone compounds suggest further effort would be warranted to optimize *in vivo* characteristics of this scaffold. Furthermore, structure-based drug design and scaffold hopping were used to transform the pyrazolopyridone core into an indazole scaffold that displayed excellent Gram-positive antibacterial activity, including good animal efficacy in several mouse infection models.[13]

■ ASSOCIATED CONTENT

Supporting Information

The Supporting Information is available free of charge on the ACS Publications website at DOI: 10.1021/acsmedchemlett.5b00368.

General procedure for GyrB and TopoIV IC_{50} determination, MIC protocol, X-ray structure determination, experimental procedure for synthesis of compounds (PDF)

■ AUTHOR INFORMATION

Corresponding Author

*Tel: 1-713-745-7499. E-mail: jbcross@mdanderson.org.

Notes

The authors declare no competing financial interest.

■ ACKNOWLEDGMENTS

The authors thank the reviewers of this manuscript for their insightful comments.

■ ABBREVIATIONS

Cipro, ciprofloxacin; Ec, *Escherichia coli*; MIC, minimum inhibitory concentration; MRSA, methicillin-resistant *Staphylococcus aureus*; MSSA, methicillin-sensitive *Staphylococcus aureus*; RI, resistance incidence; Sa, *Staphylococcus aureus*

■ REFERENCES

(1) Sanyal, G.; Doig, P. Bacterial DNA Replication Enzymes as Targets for Antibacterial Drug Discovery. *Expert Opin. Drug Discovery* **2012**, *7*, 327−339.

(2) Champoux, J. J. DNA Topoisomerases: Structure, Function, and Mechanism. *Annu. Rev. Biochem.* **2001**, *70*, 369−413.

(3) Berger, J. M.; Gamblin, S. J.; Harrison, S. C.; Wang, J. C. Structure and Mechanism of DNA Topoisomerase II. *Nature* **1996**, *379*, 225−232.

(4) Angehrn, P.; Buchmann, S.; Funk, C.; Goetschi, E.; Gmuender, H.; Hebeisen, P.; Kostrewa, D.; Link, H.; Luebbers, T.; Masciadri, R.; Nielsen, J.; Reindl, P.; Ricklin, F.; Schmitt-Hoffmann, A.; Theil, F. New Antibacterial Agents Derived from the DNA Gyrase Inhibitor Cyclothialidine. *J. Med. Chem.* **2004**, *47*, 1487−1513.

(5) Grossman, T. H.; Bartels, D. J.; Mullin, S.; Gross, C. H.; Parsons, J. D.; Liao, Y.; Grillot, A.-L.; Stamos, D.; Olson, E. R.; Charifson, P. S.; Mani, N. Dual Targeting of GyrB and ParE by a Novel Aminobenzimidazole Class of Antibacterial Compounds. *Antimicrob. Agents Chemother.* **2007**, *51*, 657−666.

(6) Charifson, P. S.; Grillot, A.-L.; Grossman, T. H.; Parsons, J. D.; Badia, M.; Bellon, S.; Deininger, D. D.; Drumm, J. E.; Gross, C. H.; LeTiran, A.; Liao, Y.; Mani, N.; Nicolau, D. P.; Perola, E.; Ronkin, S.; Shannon, D.; Swenson, L. L.; Tang, Q.; Tessier, P. R.; Tian, S.-K.; Trudeau, M.; Wang, T.; Wei, Y.; Zhang, H.; Stamos, D. Novel Dual-Targeting Benzimidazole Urea Inhibitors of DNA Gyrase and Topoisomerase IV Possessing Potent Antibacterial Activity: Intelligent Design and Evolution through the Judicious Use of Structure-Guided Design and Structure-Activity Relationships. *J. Med. Chem.* **2008**, *51*, 5243−5263.

(7) Sherer, B. A.; Hull, K.; Green, O.; Basarab, G.; Hauck, S.; Hill, P.; Loch, J. T., III; Mullen, G.; Bist, S.; Bryant, J.; Boriack-Sjodin, A.; Read, J.; DeGrace, N.; Uria-Nickelsen, M.; Illingworth, R. N.; Eakin, A. E. Pyrrolamide DNA Gyrase Inhibitors: Optimization of Antibacterial Activity and Efficacy. *Bioorg. Med. Chem. Lett.* **2011**, *21*, 7416−7420.

(8) Tari, L. W.; Trzoss, M.; Bensen, D. C.; Li, X.; Chen, Z.; Lam, T.; Zhang, J.; Creighton, C. J.; Cunningham, M. L.; Kwan, B.; Stidham, M.; Shaw, K. J.; Lightstone, F. C.; Wong, S. E.; Nguyen, T. B.; Nix, J.; Finn, J. Pyrrolopyrimidine Inhibitors of DNA Gyrase G (GyrB) and Topoisomerase IV (ParE). Part 1: Structure Guided Discovery and Optimization of Dual Targeting Agents with Potent, Broad-Spectrum Enzymatic Activity. *Bioorg. Med. Chem. Lett.* **2013**, *23*, 1529−1536.

(9) Basarab, G. S.; Manchester, J. I.; Bist, S.; Boriack-Sjodin, A.; Dangel, B.; Illingworth, R.; Sherer, B. A.; Sriram, S.; Uria-Nickelsen, M.; Eakin, A. E. Fragment-to-Hit-to-Lead Discovery of a Novel Pyridylurea Scaffold of ATP Competitive Dual Targeting Type II Topoisomerase Inhibiting Antibacterial Agents. *J. Med. Chem.* **2013**, *56*, 8712−8735.

(10) Payne, D. J.; Gwynn, M. N.; Holmes, D. J.; Pompliano, D. L. Drugs for Bad Bugs: Confronting the Challenges of Antibacterial Discovery. *Nat. Rev. Drug Discovery* **2007**, *6*, 29−40.

(11) Rees, D. C.; Congreve, M.; Murray, C. W.; Carr, R. Fragment-Based Lead Discovery. *Nat. Rev. Drug Discovery* **2004**, *3*, 660−672.

(12) Mesleh, M. F.; Cross, J. B.; Zhang, J.; Kahmann, J.; Andersen, O. A.; Barker, J.; Moy, T. I.; Yang, Q.; Shotwell, J.; Nguyen, K.; Lippa, B.; Dolle, R.; Ryan, M. D. Fragment-Based Discovery of Novel DNA Gyrase Inhibitors Targeting the ATPase Subunit of GyrB. *Bioorg. Med. Chem. Lett.* **2016**, *26*, 1314.

(13) Zhang, J.; Yang, Q.; Romero, J. A. C.; Cross, J.; Wang, B.; Poutsiaka, K. M.; Epie, F.; Bevan, D.; Wu, Y.; Moy, T.; Daniel, A.; Chamberlain, B.; Carter, N.; Shotwell, J.; Arya, A.; Kumar, V.; Silverman, J.; Nguyen, K.; Metcalf, C. A., III; Ryan, D.; Lippa, B.; Dolle, R. E. Discovery of Indazole Derivatives as a Novel Class of Bacterial Gyrase B Inhibitors. *ACS Med. Chem. Lett.* **2015**, *6*, 1080−1085.

(14) Li, X.; Tari, L. W.; Bensen, D. C.; Trzoss, M.; Lam, T.; Zhang, J.; Chen, Z.; Lee, S.-J.; Cunningham, M.; Kwan, B.; Nelson, K.; Stidham, M.; Brown-Driver, V.; Hough, G.; Phillipson, D.; Nguyen, T.; Lightstone, F.; Wong, S.; Shaw, K. J.; Finn J. Presented at the 52nd Interscience Conference on Antimicrobial Agents and Chemotherapy (ICCAC), 2012, Poster F-2017.

(15) Molecular Operating Environment (MOE), 2014.09; Chemical Computing Group Inc.: Montreal, QC, 2014.

(16) Maass, P.; Schulz-Gasch, T.; Stahl, M.; Rarey, M. ReCore: A Fast and Versatile Method for Scaffold Hopping Based on Small Molecule Crystal Structure Conformations. *J. Chem. Inf. Model.* **2007**, *47*, 390−399.

DOI: 10.1021/acsmedchemlett.5b00368
ACS Med. Chem. Lett. XXXX, XXX, XXX−XXX